J Ind Microbiol Biotechnol (2013) 40:29–39
DOI 10.1007/s10295-012-1213-y

BIOCATALYSIS

Characterization and application of a newly synthesized 2-deoxyribose-5-phosphate aldolase

Zhong-Yu You · Zhi-Qiang Liu · Yu-Guo Zheng · Yin-Chu Shen

Received: 12 July 2012 / Accepted: 2 November 2012 / Published online: 22 November 2012

Abstract A codon-optimized 2-deoxyribose-5-phosphate aldolase (DERA) gene was newly synthesized and expressed in *Escherichia coli* to investigate its biochemical properties and applications in synthesis of statin intermediates. The expressed DERA was purified and characterized using 2-deoxyribose-5-phosphate as the substrate. The specific activity of recombinant DERA was 1.8 U/mg. The optimum pH and temperature for DERA activity were pH 7.0 and 35 °C, respectively. The recombinant DERA was stable at pH 4.0–7.0 and at temperatures below 50 °C. The enzyme activity was inhibited by 1 mM of Ni^{2+}, Ba^{2+} and Fe^{2+}. The apparent K_m and V_{max} values of purified enzyme for 2-deoxyribose-5-phosphate were 0.038 mM and 2.9 μmol min^{-1} mg^{-1}, for 2-deoxyribose were 0.033 mM and 2.59 μmol min^{-1} mg^{-1}, respectively, which revealed that the enzyme had similar catalytic efficiency towards phosphorylated and non-phosphorylated substrates. To synthesize statin intermediates, the bioconversion process for production of (3*R*, 5*S*)-6-chloro-2,4,6-trideoxyhexose from chloroacetaldehyde and acetaldehyde by the recombinant DERA was developed and a conversion of 94.4 % was achieved. This recombinant DERA could be a potential candidate for application in production of (3*R*, 5*S*)-6-chloro-2,4,6-trideoxyhexose.

Keywords 2-Deoxyribose-5-phosphate aldolase · Purification · Characterization · Biotransformation · Statin intermediates

Electronic supplementary material The online version of this article (doi:10.1007/s10295-012-1213-y) contains supplementary material, which is available to authorized users.

Z.-Y. You · Z.-Q. Liu · Y.-G. Zheng (✉) · Y.-C. Shen
Institute of Bioengineering, Zhejiang University of Technology, Hangzhou 310014, Zhejiang, People's Republic of China
e-mail: zhengyg@zjut.edu.cn

Z.-Y. You · Z.-Q. Liu · Y.-G. Zheng · Y.-C. Shen
Engineering Research Center of Bioconversion and Biopurification of Ministry of Education, Zhejiang University of Technology, Hangzhou 310014, Zhejiang, People's Republic of China

Introduction

Biocatalysts are playing an important role in the chemical industry, especially in the production of chiral substances because of their attractive features including regio-, chemo-, and enantio-selectivity [30, 36]. The use of aldolases to catalyze asymmetric synthesis of complex carbohydrates is an area of great utility [4]. The enzyme, 2-deoxyribose-5-phosphate aldolase (DERA, EC 4.1.2.4), belongs to the class I aldolases and catalyzes the reversible aldol condensation reaction without any cofactors [28]. The catalytic process of its natural substrates is shown in Fig. 1a. The DERA is unique among aldolases for the acceptance of two or three aldehydes in the sequential reactions. Besides acetaldehyde, propanal, acetone and fluoroacetone are also accepted as substrates [2, 11]. The DERA has the ability to generate new chiral centers from simple materials. By using chloroacetaldehyde and acetaldehyde as substrates, DERA catalyzes the sequential aldol condensation that produces (3*R*, 5*S*)-6-chloro-2,4,6-trideoxyhexose (Fig. 1b). The chiral products obtained are important building blocks for the side chain of cholesterol-lowering drugs, such as atorvastatin and rosuvastatin etc., which are inhibitors of the 3-hydroxy-3-methyglutaryl-coenzyme A (HMG-CoA) reductase [5].

In the past few decades, a number of DERAs have been reported and characterized from different microorganisms

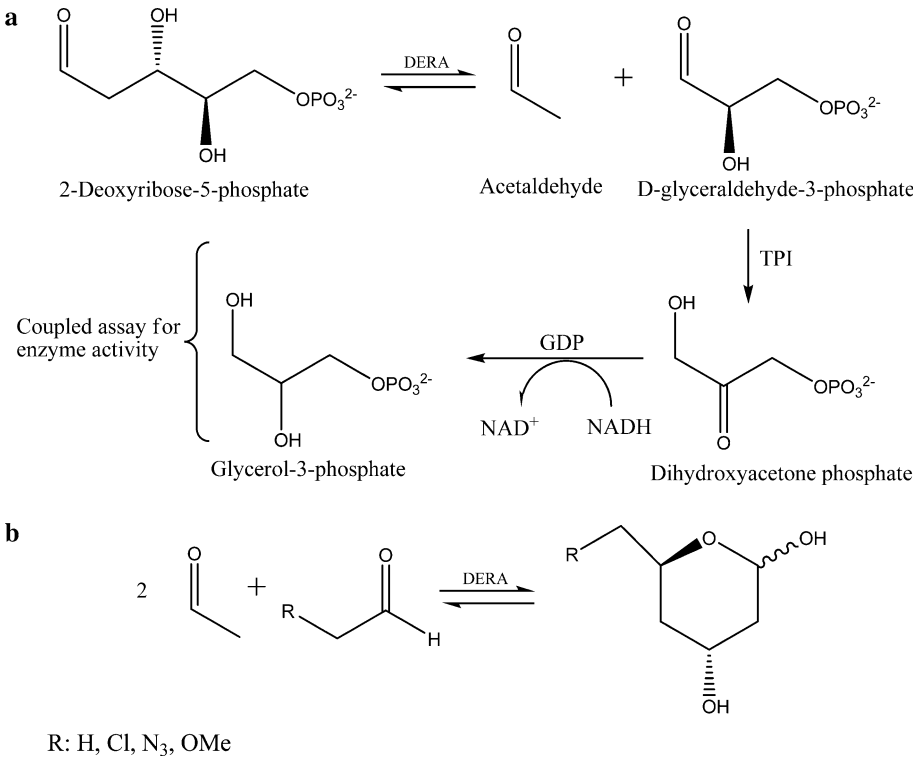

Fig. 1 Aldol-reactions catalyzed by DERA. **a** the reversible aldol condensation reaction between acetaldehyde, D-glyceraldehyde-3-phosphate and 2-deoxyribose-5-phosphate, and the steps that correspond to the coupled assay: D-glyceraldehyde-3-phosphate is converted into dihydroxyacetone phosphate by TPI, and then converted into glycerol-3-phosphate by GDP; **b** sequential aldol condensations of synthesis of (3*R*, 5*S*)-6-substituted-2, 4, 6-trideoxyhexose

including *Paenibacillus* sp. EA001 [20], *Hyperthermus butylicus* [42], *Yersinia* sp. EA015 [19], *Pyrobaculum aerophilum*, *Thermotoga maritime* [34], *Thermus thermophilus* HB8 [27], *Streptococcus mutans* GS-5 [14], *Aeropyrum pernix* [33], *Thermococcus kodakaraensis* KOD1[31] and *Escherichia coli* K12 [16], and some of their crystal structures also have been solved [16, 27, 33]. However, most of the wild type enzymes show low affinity and stability to acetaldehyde, which limits their applications. To meet with the demands of industrial applications, site-directed mutagenesis and directed evolution have been employed to improve the properties of DERA [8, 18]. The mutant enzyme S238D generated from *E.coli* DERA shows a 2.5-fold improvement in activity against the wild-type enzyme, and exhibits a larger substrate range [8, 24].

Isolation and identification of novel enzymes from the metagenome have attracted much more attention in recent years [10, 21]. A novel DERA has been identified from environmental DNA libraries by using a high-throughput screening method [13]. In addition, an aldolase-catalyzed process for enantioselective synthesis of (3*R*, 5*S*)-6-chloro-2,4,6-trideoxyhexose utilizing this enzyme has been constructed [13]. However, the biochemical properties and three-dimensional (3D) structure of this DERA have not been reported. To elaborate the biochemical properties of this enzyme for the purpose of further understanding its functions in the aldol reaction, the DERA gene was synthesized after codons optimization and then successfully expressed in *E. coli* BL21 (DE3). After purification using nickel column, the catalytic properties of the recombinant DERA and its applications for synthesis of statin intermediates were investigated.

Materials and methods

Bacterial strain, plasmid and growth conditions

E. coli BL21 (DE3) and plasmid pET-28b were used for overexpression of the recombinant protein. Cells were grown in standard Luria–Bertani (LB) medium composed of (g/L): yeast extract (5), peptone (10) and NaCl (10) [35]. If necessary, kanamycin (Kan) with a concentration of 50 μg/mL was supplemented into the medium. Incubations were carried out at 37 °C on a rotary shaker at 150 rpm.

Synthesis and cloning of DERA gene

The amino acid sequence of DERA was obtained from the previous report [13]. The nucleotide sequence encoding this enzyme was optimized for improved expression in *E. coli* by software [40]. To purify the protein, we introduced a 6 × his-tag into the C-terminus of the enzyme. The optimized nucleotide sequence was deposited in the GenBank database under accession number JX124232. The complete sequence was synthesized by the PCR assembly

method [32], and cloned into the pET-28b vector. Subsequently, the recombinant plasmid, designated pET-28b-DERA, was transformed into *E. coli* BL21 (DE3) competent cells using the heatshock method [3].

Expression and purification of recombinant DERA

E. coli BL21 (DE3) harboring the plasmid pET-28b-DERA were cultivated in LB medium with Kan at 37 °C on a rotary shaker (150 rpm). The expression of DERA was induced when the optical density reached 0.6–0.8 at 600 nm by the addition of isopropyl β-D-1-thiogalactopyranoside (IPTG) to a final concentration of 0.1 mM for 8 h at 28 °C. Cells were collected by centrifugation at 4 °C, 8,000×*g* for 10 min, subsequently washed with 50 mM phosphate buffer (pH 7.4) twice, and then stored at −80 °C.

The purification procedure was performed on the ÄKTA^{TM} explorer system (Amersham Biosciences Corp., Uppsala, Sweden) with a 16 mmD/100 mmL POROS MC 20 μm column (Applied Biosystems Co., USA). The cell pellet was solubilized in 50 mM NaH_2PO_4 buffer with 0.5 mM imidazole (pH 8.0), then disrupted by sonication for a period of 10 min on ice. After centrifuging at 4 °C, 16,000×*g* for 20 min, the supernatant was filtered by a 0.45 μm filter, and loaded onto the column (chelated with Ni^{2+}). Approximately two column volumes (CVs) of 50 mM NaH_2PO_4 buffer containing 50 mM imidazole and 500 mM NaCl were run to wash out any proteins that were bound nonspecifically to the column [25]. The recombinant DERA was eluted with a linear gradient of 50–500 mM imidazole in 50 mM phosphate buffer (pH 8.0) containing 500 mM NaCl. The samples were dialyzed overnight against deionized water and then freeze-dried. The purified recombinant protein was analyzed by sodium dodecyl sulfate–polyacrylamide gel electrophoresis (SDS-PAGE) [22].

SDS-PAGE electrophoresis

The purity and molecular mass of the recombinant DERA were determined by SDS-PAGE. The SDS-PAGE was performed on a 5 % (w/v) acrylamide stacking gel and 12 % (w/v) separating gel using a Mini-gel system (Bio-Rad) as described by Laemmli [22]. The gels were cast with 0.75 mm spacers (Bio-Rad). The samples were mixed with an equal volume of 2 × loading buffer and heated at 100 °C for 10 min before electrophoresis. The gels were stained with dye solution (0.1 % Coomassie brilliant blue R-250 in 45 % ethanol and 10 % acetic acid) and destained with solution containing 10 % ethanol and 10 % acetic acid. A wide molecular range (10–170 kDa) protein standard (Fermentas International Inc., Shenzhen, China) was used as molecular mass marker.

Enzyme activity and protein concentration

The DERA activity was determined by a coupled enzymatic system which contained 20 mM Na_2HPO_4-citric acid buffer (pH 7.0), 1 mM substrate (2-deoxyribose-5-phosphate (DRP) or 2-deoxyribose (DR)), 0.5 mM NADH, 6 U triose-phosphate isomerase (EC 5.3.1.1, TPI), 2 U glycerophosphate dehydrogenase (EC 1.1.1.8, GDP) and 10 μL diluted DERA in a 200 μL total volume. The reaction was carried out at 35 °C for 30 min. In this reaction DRP is converted into glycerol-3-phosphate by DERA, TPI and GDP (Fig. 1a). The decrease in absorbance due to the consumption of NADH was measured at 340 nm using a universal microplate spectrophotometer (Spectramax plus,Molecular Devices, USA). The consumption of one molecule of NADH was corresponded to the decomposition of one molecule of DRP. One enzyme unit (U) is defined as the amount of enzyme catalyzing the cleavage of 1 μmol of substrate per minute under the assay conditions. All activity measurements were performed in triplicate.

The protein concentration was quantified by using the bicinchoninic acid (BCA) protein assay kit (Nanjing Keygen Biotechnology Co., China) based on the reported method [38]. The assay was carried out according to the manufacturer's instructions.

Effects of pH and temperature on activities and stabilities of DERA

The effects of pH on DERA activities were measured using DRP as substrate in the pH range of 3.0–11.0. The reactions at each pH were conducted at 28 °C and the relative activities were tested. The following buffers were used with a concentration of 20 mM: Citric acid-sodium citrate buffer (pH 3.0–5.0), Na_2HPO_4-citric acid buffer (pH 5.0–7.0), Tris–HCl buffer (pH 7.0–9.0) and K_2HPO_4–KOH buffer (pH 9.0–11.0). The pH stabilities of DERA were examined by incubating the enzyme at 25 °C in buffers at pH values ranging from 3.0–10.0 for 5 h. The residual activities were determined under the standard conditions as described above. The non-incubated enzyme was taken as a control.

The effects of temperature on DERA activities were investigated from 20 to 60 °C. The reactions were carried out at various temperatures in 200 μL solution containing Na_2HPO_4-citric acid buffer (20 mM, pH 7.0), 1 mM of DRP and diluted DERA. After 30 min DERA was removed by centrifugation using a centrifugal filter device (Millipore, USA). Then the coupled enzymatic reaction was carried out by adding NADH, TPI and GDP at 35 °C. The thermal stabilities were measured by incubating the enzyme at temperatures ranging from 20 to 70 °C for 10 min and the remaining activities were determined under the standard

conditions as described above. The non-incubated enzyme was taken as a control.

Circular dichorism (CD) spectroscopy

CD analysis was performed using a JASCO J-815 Spectropolarimeter (Jasco Inc., Japan) and quartz suprasil cuvettes of 10 mm path length. The DERA was analyzed at a concentration of 0.1 mg/mL in 20 mM Tris–HCl (pH 8.0). The spectra for DERA were collected in triplicate at wavelengths from 190 to 300 nm with a scan speed of 20 nm/min. Spectra manager 228 software was used for data acquisition.

Effects of metal ions on enzyme activities

The effects of metal ions on enzyme activities were studied by pre-incubating the enzyme with different metal ions including Ag^{+}, Li^{+}, Cu^{2+}, Ni^{2+}, Mn^{2+}, Ca^{2+}, Mg^{2+}, Zn^{2+}, Ba^{2+}, Co^{2+} and Fe^{2+} with a final concentration of 1 mM at 25 °C for 30 min. The residual activities were measured under the standard conditions using DRP as the substrate. The activity in the absence of metal ions was recorded as 100 %.

Kinetic analysis

Kinetic parameters were calculated from the initial rates of reactions catalyzed by the purified enzymes under standard assay conditions. The DRP and DR were used as substrates with concentrations ranging from 0.01 to 1 mM. The initial rates obtained were fitted to the equation: $V = V_{max}\cdot[S]/(K_m + [S])$, where V_{max} is the maximum rate, [S] is the substrate concentration, and K_m is the Michaelis constant.

Application of the recombinant DERA in synthesis of statin intermediates

Biotransformation was performed at 35 °C using the purified DERA in a 50-mL conical flask. The reaction mixture consisted of 25 mg of DERA, 10 mL of 100 mM Na_2HPO_4-citric acid buffer (pH 7.0), 240 mM acetaldehyde or 80 mM chloroacetaldehyde and 160 mM acetaldehyde as substrates. Samples were withdrawn at regular intervals, and measured by gas chromatography (Agilent 7890A system) equipped with a flame ionization detector and a HP-5 capillary column (30 m × 0.32 mm, 0.25 μm film thickness, 5 % Phenyl/95 % dimethylpolysiloxane). Nitrogen was used as carrier gas at a flow rate of 1.0 mL/min. The column temperature was held for 4 min at 80 °C, elevated at 20 °C/min to 220 °C, and held for 4 min at 220 °C. Temperatures of both inlet and detector were set at 250 °C. The conversion was calculated using the following formula: conversion (%) = $M_c/M_s \times 100$ %, where M_c is the mole of acetaldehyde consumed and M_s is the mole of acetaldehyde supplied.

Modeling and molecular docking

Build Homology Models (MODELER) module in Discovery Studio (DS) 2.1 (Accelrys, Inc., USA) was used for predicting the 3D structure of DERA. The crystal structures of DERAs from *Entamoeba histolytica* (PDB accession NO. 3NGJ) and *Thermotoga maritima* (PDB accession NO. 3R12) were used as templates. Pairwise alignment of DERA and template sequences were done using the program ClustalX [39], and the picture of the sequence alignment was made by the program ESPRIPT [12]. The generated structures were improved by subsequent refinement of the loop conformations by assessing the compatibility of an amino acid sequence to the known PDB structures using the Protein Health module in DS 2.1. Molecular docking was performed using Autodock 4.0.1 software [29]. Protein structure and ligand–protein interaction diagrams were prepared with PyMOL [7] and Ligplot [23].

Results

Expression and purification of recombinant DERA

Based on the reported amino acid sequence of DERA [13], the DERA gene was synthesized after codons optimization. The total length of the synthesized gene is 681 bp, encoding a 23.9-kDa protein. The gene was inserted into the pET-28b vector between the *Nco*I and *Sal*I sites to construct recombinant plasmid pET-28b-DERA, and then the recombinant plasmid was transformed into *E.coli* BL21 (DE3). Colonies were picked up and the recombinant plasmids were extracted and further sequenced to verify the existence of the DERA gene.

The *E. coli* BL21 (DE3) harboring pET-28b-DERA was incubated in LB medium and induced by the addition of 0.1 mM IPTG at OD_{600} of 0.6–0.8. The recombinant DERA was expressed with 6 × his-tag at the C-terminus which led to a simplified method for purification of the protein using immobilized metal-chelating affinity chromatography (IMAC) in one-step. Table 1 summarizes the results of the purification process. The recombinant DERA was purified 2.3 times with a yield of 56.3 %. The specific activity of purified enzyme towards DRP was 1.8 U/mg. The purified DERA appeared as a single protein band on SDS-PAGE gel with a molecular mass of approximately 24 kDa (Fig. S1 in the supplementary material).

Table 1 Summary of the purification of recombinant DERA

Purification step	Total protein (mg)	Total activity (U)	Specific activity (U/mg)	Purification (fold)	Yield (%)
Crude enzyme	312.0	249.6	0.8	1.0	100
Ni–NTA affinity chromatography	78.1	140.5	1.8	2.3	56.3

Optimal pH for activity and pH stability

The pH-activity profiles of the purified DERA were determined. The specific pH was controlled by different buffer systems. The enzyme was optimally active at pH 7.0 in 20 mM Na_2HPO_4-citric acid buffer (Fig. 2a), and it showed high relative activities (above 90 %) in a pH range of 6.0–8.0 in Na_2HPO_4-citric acid or Tris–HCl buffer. The pH stability showed that the enzyme was stable over a broad pH range of 4.0–7.0 with more than 80 % residual activities after incubation for 5 h (Fig. 2b).

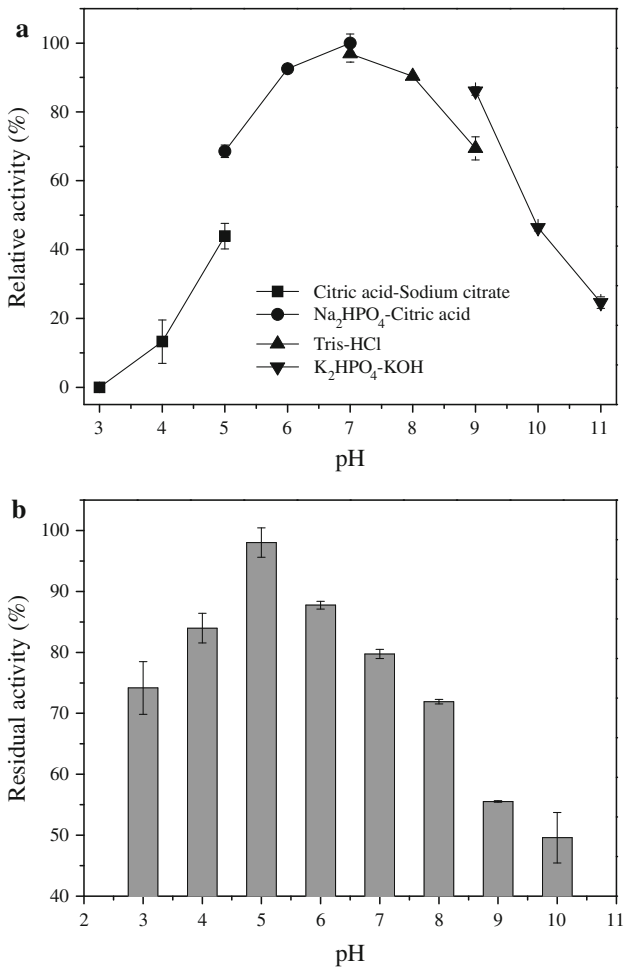

Fig. 2 Effects of pH on the activities (**a**) and stabilities (**b**) of the recombinant DERA. Optimal pH for activity was determined by measuring cleavage of the DRP in buffers of various pH values at 28 °C for 30 min. The enzyme activity obtained in 20 mM Na_2HPO_4-citric acid buffer (pH 7.0) was taken as 100 %. The pH stability was assessed under optimal conditions after the enzyme had been incubated in various buffers for 5 h. The non-incubated enzyme was taken as a control

Optimal temperature for activity and thermostability

To evaluate the effects of temperature on enzyme activities, the enzymes were incubated at various temperatures. The purified DERA was active between 20 and 60 °C with an optimum around 35 °C, and the activity decreased sharply above 50 °C (Fig. 3a). The DERA thermostability was investigated by analyzing the residual activities after incubation at different temperatures. It was fairly stable up to 50 °C and showed 63 % of initial activity after 10 min incubation at 55 °C (Fig. 3b).

It is known that CD spectroscopy is a useful tool not only in the determination of protein secondary structures, but also in the investigation of enzyme thermostability [41]. Minor structural alterations can be described by CD spectroscopy, not necessarily involving large enthalpy changes. We recorded the CD spectra of DERA at different temperatures (Fig. 3c). The spectra showed little changes at temperatures between 10 to 50 °C, indicating that no substantial changes were occurring in the secondary structure of protein at these temperatures. The spectrum at 55 °C was changed as associated with the conformational changes of protein. There were observable changes in the CD spectra at 60, 65 and 70 °C. This result is consistent with enzyme activity that decreased rapidly after incubation at temperatures higher than 55 °C.

Effects of metal ions on the activities of recombinant DERA

The effects of different metal ions on the activities of purified DERA were tested by incubating the enzyme in the presence of reagents at 25 °C for 30 min. The residual activities were assayed according to the standard method. As shown in Table 2, the majority of metal ions did not significantly affect the activities of purified DERA except Ni^{2+}, Ba^{2+} and Fe^{2+}, which slightly inhibited the enzyme activities. The metal chelator EDTA also did not inhibit the enzyme activity, indicating that this enzyme is not a metalloenzyme.

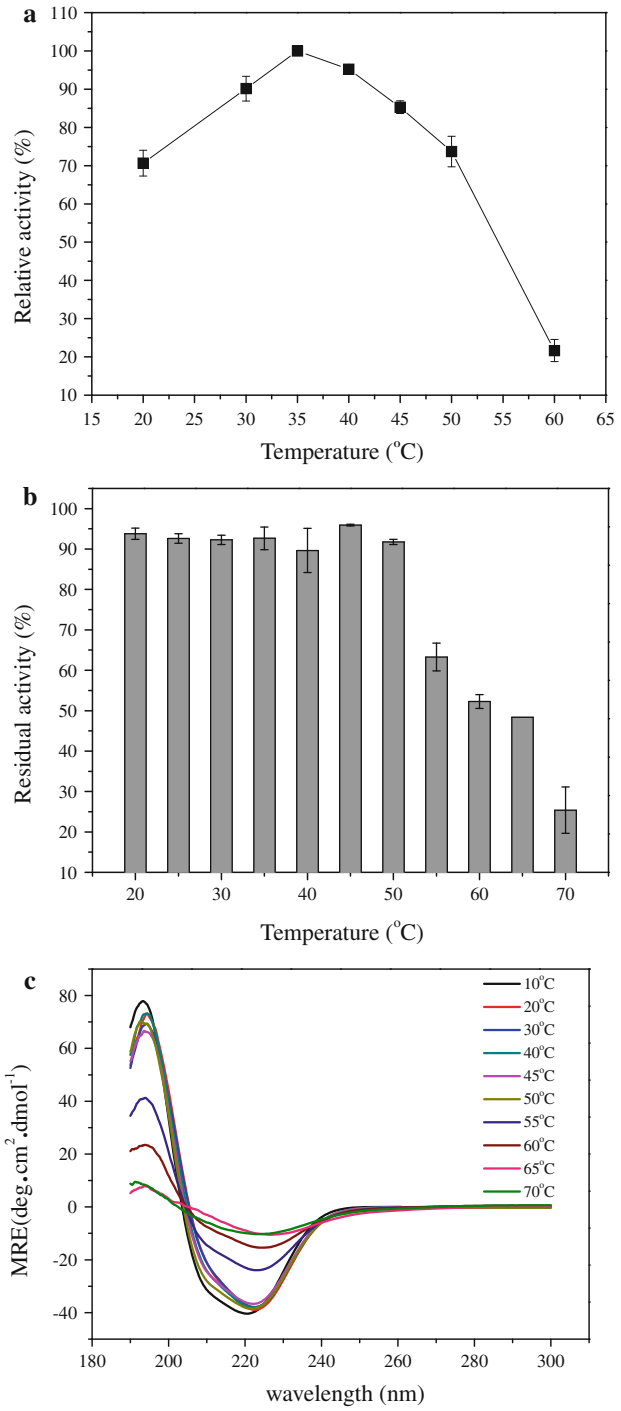

Fig. 3 Effects of temperature on the recombinant DERA. **a** activity; **b** thermostability; **c** circular dichroism analysis. Optimal temperature for activity was determined by measuring cleavage of the DRP in 20 mM Na_2HPO_4-citric acid buffer (pH 7.0) at various temperatures for 30 min. The value obtained at 35 °C was taken as 100 %. Thermostability was assayed under optimal conditions after the enzyme had been incubated at various temperatures for 10 min. The non-incubated enzyme was taken as control. The CD spectra of DERA were collected in triplicate at wavelengths from 190 to 300 nm with a scan speed of 20 nm/min (color figure online)

Table 2 Effects of metal ions and EDTA on the activities of recombinant DERA

Metal ions	Relative activity (%)[a]	Metal ions	Relative activity (%)[a]
Control	100 ± 3.1	Mg^{2+}	95 ± 2.7
Ag^{+}	102 ± 7.2	Zn^{2+}	95 ± 0.5
Li^{+}	91 ± 3.1	Ba^{2+}	83 ± 0.3
Cu^{2+}	93 ± 0.3	Co^{2+}	99 ± 2.1
Ni^{2+}	84 ± 5.0	Fe^{2+}	74 ± 7.9
Mn^{2+}	96 ± 0.3	EDTA	102 ± 3.0
Ca^{2+}	92 ± 1.5		

[a] The enzyme activity was measured under the standard conditions using DRP as substrate after incubating the enzyme with different metal ions with a final concentration of 1 mM at 25 °C for 30 min. The activity in the absence of metal ions was recorded as 100 %

Determination of kinetic parameters

The kinetic behaviors of DERA towards DRP and DR can be reasonably well described by the Michaelis–Menten model. The results show the typical Michaelis–Menten type kinetics for enzyme activities with increasing DRP and DR concentrations (Fig. S2 in the supplementary material). The K_m and V_{max} values of purified enzyme for DRP were 0.038 mM and 2.9 μmol min^{-1} mg^{-1}, for DR they were 0.033 mM and 2.59 μmol min^{-1} mg^{-1}, respectively.

Time course of synthesis of statin intermediates

The biosynthesis of statin intermediates was executed by the recombinant DERA using different substrates. The time courses of reactions under optimum conditions were measured. As shown in Fig. 4a, when acetaldehyde and chloroacetaldehyde were used as substrates the conversion reached 94.4 %, which was higher than that of the reaction using acetaldehyde only. This indicated that DERA can catalyze the sequential aldol condensation between the same aldehydes, and the introduction of some aldehydes derivatives will promote the reaction.

Sequence analysis, homology modeling and molecular docking

The Basic Local Alignment Search Tool (BLAST) was executed in the Genbank database for the identification of the DERA amino acid sequence in this study. It showed 90.9, 76.0 and 73.3 % identities to the DERAs from *Geobacillus thermodenitrificans* NG80-2 (Genbank accession No. ABO67780) [9], *Anoxybacillus flavithermus* WK1 (Genbank accession No. YP_002317118) [37] and *Bacillus cereus* Rock3-44 (Genbank accession No. ZP_04219039),

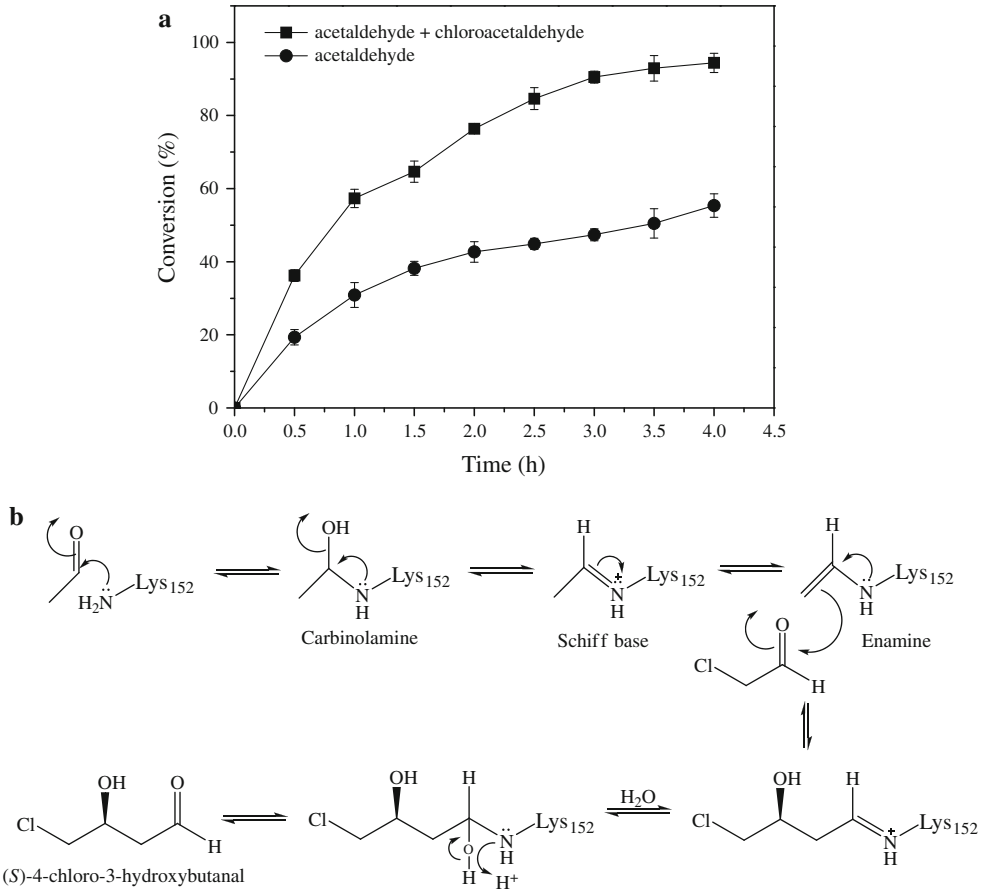

Fig. 4 **a** the time course of aldol reaction using DERA. The reaction was performed at 35 °C using the purified DERA. 25 mg of DERA was incubated with 10 mL of 100 mM Na_2HPO_4-citric acid buffer (pH 7.0), 240 mM acetaldehyde or 80 mM chloroacetaldehyde and 160 mM acetaldehyde; **b** the catalytic mechanism of DERA to catalyze sequential aldol condensation between acetaldehyde and chloroacetaldehyde

respectively. An alignment of these amino acid sequences is shown in Fig. 5. The residues in active sites including Lys152, Thr155, Ser183, Gly184, Gly185, Gly204, Thr205 and Ser206 are very conservative.

The secondary and 3D structures of DERA were generated using experimentally determined protein structures as templates that had high sequence identity with the DERA obtained in this study. A BLAST search in the Protein Data Bank showed that this DERA was quite similar to the DERAs from *Entamoeba histolytica* (58.7 % identity; PDB accession no. 3NGJ, resolution 1.70 Å) and *Thermotoga maritima* (54.3 % identity; PDB accession no. 3R12, resolution 1.75 Å). According to the homology analysis, this DERA is consisted of ten α-helices and eight β-sheets. It is the same conclusion with CD spectra (data not shown) that showed the purified DERA appeared to be richer in α-helix than in β-sheet. Figure 6a displays the best quality model of this DERA. It contains a TIM $(\alpha/\beta)_8$ barrel fold, which is the typical structure of class I aldolases [16]. Molecular docking was further carried out to deeply understand the interactions between substrates and residues in the active site. The results showed that DRP and DR were successfully docked into the active site of the enzyme (Fig. 6b, c) with different docked energy, −1.55 and −1.45 kcal/mol, respectively. In addition, for predicting the best substrate for the production of statin intermediates, acetaldehyde, chloroacetaldehyde, fluoacetaldehyde, bromoacetaldehyde, propionaldehyde and 3-azidopropinaldehyde were also investigated in molecular docking and their docked energies were −2.16, −1.95, −1.57, −2.43, −2.3 and −2.73 kJ/mol, respectively. Moreover, the distance between the carbonyl of 3-azidopropinaldehyde and the catalytic residue Lys152 was shortest (data not shown).

Discussion

The 2-deoxyribose-5-phosphate aldolase has received considerable attention due to its ability to form carbon–carbon bonds and generate new chiral centers using simple materials. A DERA with high ability to synthesize (3*R*, 5*S*)-6-chloro-2,4,6-trideoxyhexose, the chiral building block for side chain of statins, was isolated from environmental DNA libraries [13]. However, the properties of this enzyme have not been well studied. In the present study, we focused on the information on the bio-characteristics and catalytic mechanism of this enzyme to explore its new applications.

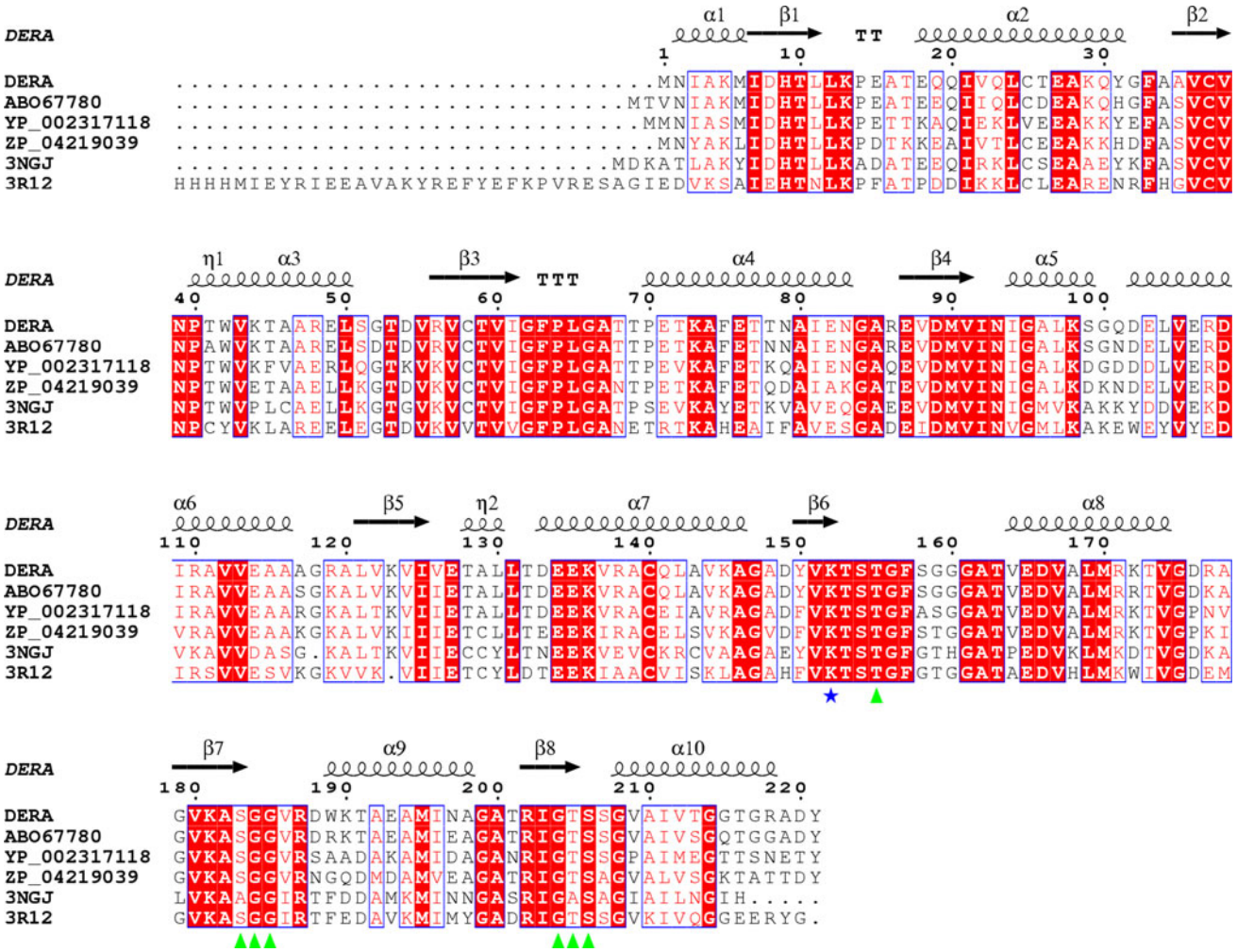

Fig. 5 Multiple sequence alignment of DERA with proteins from different sources: sequences of *Geobacillus thermodenitrificans* NG80-2 (ABO67780), *Anoxybacillus flavithermus* WK1 (YP_002317118), *Bacillus cereus* Rock3-44 (ZP_04219039), *Entamoeba histolytica* (3NGJ) and *Thermotoga maritime* (3R12). Conserved residues are *shaded in red background*. Residues in the active site are shown in *green triangles*. The catalytic residue is shown in *blue star*. The schematic diagram of secondary structure of DERA is shown on the top of sequence. The α-helices are displayed as squiggles, β-sheets as *arrows*, strict β turns as TT letters and strict α turns as TTT (color figure online)

The DERA gene was optimized and synthesized, placed under the control of the bacteriophage T7 RNA polymerase promoter and expressed in *E. coli*. After purification, the biochemical properties of this DERA were investigated and compared with that of various DERAs from a number of different microorganisms (Table 3). The pH is known to affect activities, stabilities and biotransformation performances of enzymes. In comparison, the optimum pH of this recombinant DERA (pH 7.0) is higher than DERAs from other sources except the enzyme from *E. coli* that shows the highest activity at pH 7.5. Otherwise, the DERA in this study is more active over a broader pH range (above 90 % relative activity in pH range of 6.0–8.0) than other reported enzymes. It is reported that DERA from *Yersinia* sp. EA015 displayed optimal activity at 6.0, retained about 60 % of its maximum activity at pH 7.0 and completely lost its activity at pH 5.0 [19]. The optimum temperature of the recombinant DERA (35 °C) is lower than that of DERAs from other known microorganisms, which display maximum activity at temperatures between 50 and 95 °C. It means that the biotransformation using this recombinant DERA can be occurring under milder conditions (neutral pH, lower temperature) which are expected in industrial applications. In addition, the K_m value of this DERA for DRP (0.038 mM) is lower than those of most DERAs from other sources, which range from 0.02 to 145 mM. The similar K_m values and docked energies of this DERA towards DRP and DR indicate that this enzyme has almost the same affinity with phosphorylated and non-phosphorylated substrates.

Compared with other wild-type DERAs, the DERA obtained in this study shows a greater catalytic efficiency in

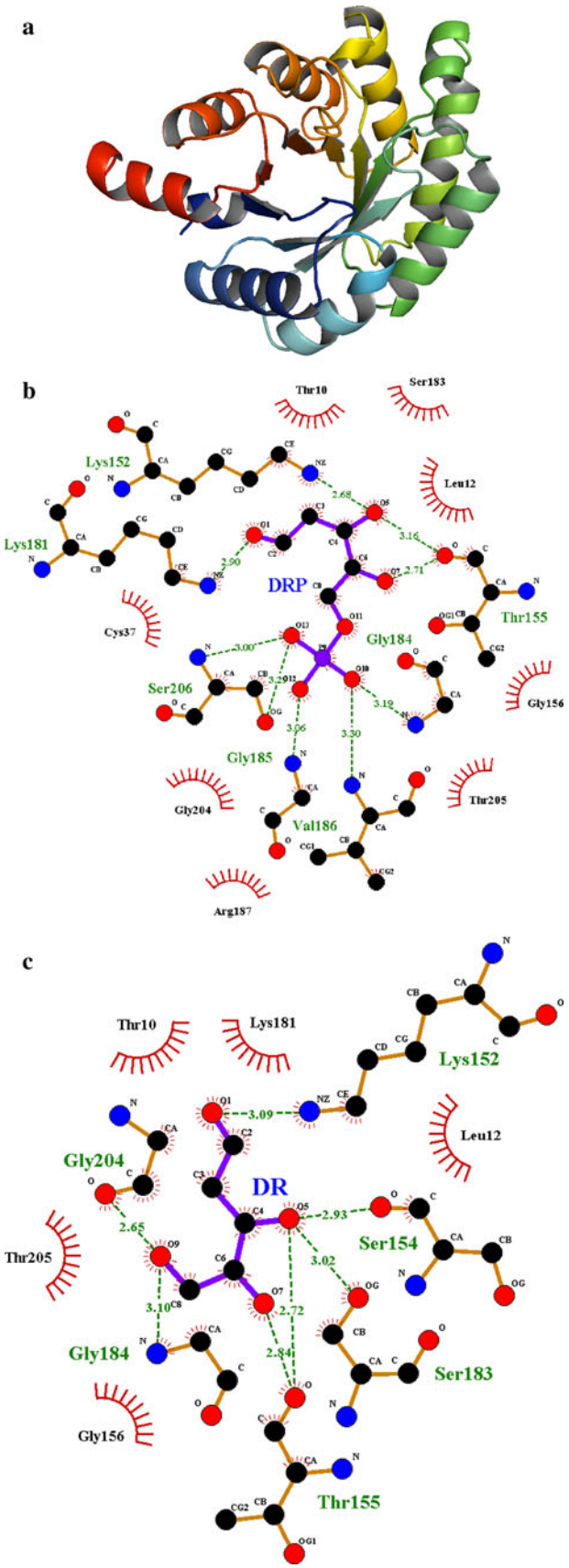

◀ **Fig. 6** Homology modeling and molecular docking. **a** Homology protein model of DERA. **b** DRP docking into the active site of the enzyme. **c** DR docking into the active site of the enzyme

aldol reactions. This DERA needed only 4 h to complete the aldol reactions (94.4 % of conversion) with an aldehyde group concentration of 240 mM, while the DERAs from *P. aerophilum*, *T. maritima* and *E. coli* needed at least 20 h [34]. This DERA also shows certain advantages even compared with mutant S238D and DERA^{Var9}, which afforded a yield of 35–43 % and a conversion of 86 %, respectively, in the sequential aldol condensation [18, 24]. The distinguishing characteristics and performances in the sequential aldol condensation taken together suggest that the DERA in the present study may have potential in the production of statin intermediates. However, to meet with the requirements for its upscale applications, the specific activity of this DERA is still needing to be improved by protein engineering techniques such as structure-based mutagenesis [17], by which the mutant S238D with 2.5 fold higher activity was constructed [8]. Based on the investigation of structure modeling and molecular docking, site-directed mutagenesis at specific sites of the recombinant DERA, such as Ser206 which corresponds to Ser238 of *E. coli* DERA, may improve the properties of the enzyme. In addition, other protein engineering techniques such as error-prone PCR, DNA shuffling [26] can also be used to promote the enzyme properties.

Computerized protein modeling and molecular docking analysis can provide the relationship between structure and function of an enzyme [1]. In this study, we found that Lys152 of this DERA was the catalytic residue consistent with Lys167 of *E. coli* DERA [15]. The catalytic mechanism of DERA to catalyze the sequential aldol condensation between acetaldehyde and chloroacetaldehyde can be proposed as follows (Fig. 4b): the catalytic residue Lys152 attacks the carbonyl of acetaldehyde to form a carbinolamine. The carbinolamine subsequently collapses to a Schiff base and tautomerizes to an enamine group and then attacks the carbonyl of chloroacetaldehyde. After hydrolysis and release of the enzyme, the (*S*)-4-chloro-3-hydroxybutanal is formed. Another acetaldehyde goes through the same process, the product (3*R*, 5*S*)-6-chloro-2, 4, 6-trideoxyhexose is formed finally [6, 16]. It is reported that the R groups (Fig. 1b) of aldehydes have a great influence on the aldol reaction [24]. In this study, the difference in docked energies between chloroacetaldehyde and acetaldehyde could contribute to a better understanding of the phenomenon that it was more efficient when chloroacetaldehyde was involved in the reaction. Otherwise, 3-azidopropinaldehyde showed the lowest docked energy and shortest distance between its carbonyl and Lys152 in

Table 3 Comparison of DERAs from various organisms

Source	Molecular mass (kDa)	Optimum pH	Optimum temperature (°C)	K_m^a (mM)	Specific activity or V_{max}^a (μmol min^{-1} mg^{-1})	References
Environmental sample	23.9	7.0	35	0.038	2.9	This study
Paenibacillus sp. EA001	24.5	6.0	50	145	62	[20]
H. butylicus	26.4	5.5	80	0.15	0.5	[42]
Yersinia sp. EA015	24.8	6.0	50	9.1	137	[19]
P. aerophilum	24.5	5.5	NS	0.066	0.25	[34]
T. maritima	27.8	6.5	NS	0.02	1.0	[34]
E. coli	28	7.5	NS	0.23	58	[34]
A. pernix	24.5	6.5	NS	0.057	4.5	[33]
T. kodakaraensis	25	4.0	95	0.81	235	[31]

[a] These values were measured by using DRP as substrate. *NS* not specified

all aldehydes tested. Therefore, we deduce that 3-azidopropinaldehyde may be the best substrate for the sequential aldol condensation of synthesis of statin intermediates.

In conclusion, this work describes the recombinant expression, purification and characterization of a novel DERA. The 3D structure and catalytic mechanism of this DERA are also described. This fundamental research has laid a foundation for applications of this enzyme. Further work will focus on the modification of the enzyme by rational or irrational protein design methods, which is ongoing in our lab.

Acknowledgments The supports of this work by the National Basic Research Program of China (973 Program) (No. 2011CB710806), Natural Science Foundation of Zhejiang Province (No. R3110155), National High Technology Research and Development Program of China (863 Program) (No. 2011AA02A210) and Qianjiang Talent Project of Zhejiang Province are gratefully acknowledged.

References

1. Baker PJ, Poultney C, Liu ZQ, Gross R, Montclare JK (2012) Identification and comparison of cutinases for synthetic polyester degradation. Appl Microbiol Biotechnol 93(1):229–240
2. Chen LR, Dumas DP, Wong CH (1992) Deoxyribose-5-phosphate aldolase as a catalyst in asymmetric aldol condensation. J Am Chem Soc 114(2):741–748
3. Chung CT, Niemela SL, Miller RH (1989) One-step preparation of competent *Escherichia coli*: transformation and storage of bacterial cells in the same solution. Proc Natl Acad Sci USA 86(7):2172–2175
4. Clapes P, Fessner WD, Sprenger GA, Samland AK (2010) Recent progress in stereoselective synthesis with aldolases. Curr Opin Chem Biol 14(2):154–167
5. Corsini A, Maggi FM, Catapano AL (1995) Pharmacology of competitive inhibitors of HMG-CoA reductase. Pharmacol Res 31(1):9–27
6. Dean SM, Greenberg WA, Wong CH (2007) Recent advances in aldolase-catalyzed asymmetric synthesis. Adv Synth Catal 349(8–9):1308–1320
7. DeLano WL (2002) The PyMOL user's manual. DeLano Scientific, San Carlos
8. DeSantis G, Liu JJ, Clark DP, Heine A, Wilson IA, Wong CH (2003) Structure-based mutagenesis approaches toward expanding the substrate specificity of D-2-deoxyribose-5-phosphate aldolase. Bioorgan Med Chem 11(1):43–52
9. Feng L, Wang W, Cheng JS, Ren Y, Zhao G, Gao CX, Tang Y, Liu XQ, Han WQ, Peng X, Liu RL, Wang L (2007) Genome and proteome of long-chain alkane degrading *Geobacillus thermodenitrificans* NG80-2 isolated from a deep-subsurface oil reservoir. Proc Natl Acad Sci USA 104(13):5602–5607
10. Fernandez-Arrojo L, Guazzaroni ME, Lopez-Cortes N, Beloqui A, Ferrer M (2010) Metagenomic era for biocatalyst identification. Curr Opin Biotechnol 21(6):725–733
11. Gijsen HJM, Wong CH (1994) Unprecedented asymmetric aldol reactions with 3 aldehyde substrates catalyzed by 2-deoxyribose-5-phosphate aldolase. J Am Chem Soc 116(18):8422–8423
12. Gouet P, Courcelle E, Stuart DI, Metoz F (1999) ESPript: analysis of multiple sequence alignments in PostScript. Bioinformatics 15(4):305–308
13. Greenberg WA, Varvak A, Hanson SR, Wong K, Huang HJ, Chen P, Burk MJ (2004) Development of an efficient, scalable, aldolase-catalyzed process for enantioselective synthesis of statin intermediates. Proc Natl Acad Sci USA 101(16):5788–5793
14. Han TK, Zhu Z, Dao ML (2004) Identification, molecular cloning, and sequence analysis of a deoxyribose aldolase in *Streptococcus* mutans GS-5. Curr Microbiol 48(3):230–236
15. Heine A, DeSantis G, Luz JG, Mitchell M, Wong CH, Wilson IA (2001) Observation of covalent intermediates in an enzyme mechanism at atomic resolution. Science 294(5541):369–374
16. Heine A, Luz JG, Wong CH, Wilson IA (2004) Analysis of the class I aldolase binding site architecture based on the crystal structure of 2-deoxyribose-5-phosphate aldolase at 0.99 angstrom resolution. J Mol Biol 343(4):1019–1034
17. Hlima HB, Aghajari N, Ali MB, Haser R, Bejar S (2012) Engineered glucose isomerase from *Streptomyces* sp. SK is resistant to Ca^{2+} inhibition and Co^{2+} independent. J Ind Microbiol Biotechnol 39(4):537–546
18. Jennewein S, Schurmann M, Wolberg M, Hilker I, Luiten R, Wubbolts M, Mink D (2006) Directed evolution of an industrial biocatalyst: 2-deoxy-D-ribose 5-phosphate aldolase. Biotechnol J 1(5):537–548
19. Kim YM, Chang YH, Choi NS, Kim Y, Song JJ, Kim JS (2009) Cloning, expression, and characterization of a new deoxyribose 5-phosphate aldolase from *Yersinia* sp EA015. Protein Expres Purif 68(2):196–200
20. Kim YM, Choi NS, Kim YO, Son DH, Chang YH, Song JJ, Kim JS (2010) Expression and characterization of a novel deoxyribose 5-phosphate aldolase from *Paenibacillus* sp. EA001. J Microbiol Biotechnol 20(6):995–1000

21. Ko KC, Rim SO, Han Y, Shin BS, Kim GJ, Choi JH, Song JJ (2012) Identification and characterization of a novel cold-adapted esterase from a metagenomic library of mountain soil. J Ind Microbiol Biotechnol 39(5):681–689
22. Laemmli UK (1970) Cleavage of structural proteins during the assembly of the head of bacteriophage T4. Nature 227(5259): 680–685
23. Laskowski RA, Swindells MB (2011) LigPlot+: multiple ligand-protein interaction diagrams for drug discovery. J Chem Inf Model 51(10):2778–2786
24. Liu JJ, Hsu CC, Wong CH (2004) Sequential aldol condensation catalyzed by DERA mutant Ser238Asp and a formal total synthesis of atorvastatin. Tetrahedron Lett 45(11):2439–2441
25. Liu ZQ, Gosser Y, Baker PJ, Ravee Y, Lu Z, Alemu G, Li H, Butterfoss GL, Kong XP, Gross R, Montclare JK (2009) Structural and functional studies of *Aspergillus oryzae* cutinase: enhanced thermostability and hydrolytic activity of synthetic ester and polyester degradation. J Am Chem Soc 131(43):15711–15716
26. Liu ZQ, Sun ZH, Leng Y (2006) Directed evolution and characterization of a novel D-pantonohydrolase from *Fusarium moniliforme*. J Agric Food Chem 54(16):5823–5830
27. Lokanath NK, Shiromizu I, Ohshima N, Nodake Y, Sugahara M, Yokoyama S, Kuramitsu S, Miyano M, Kunishima N (2004) Structure of aldolase from *Thermus thermophilus* HB8 showing the contribution of oligomeric state to thermostability. Acta Crystallogr D 60:1816–1823
28. Machajewski TD, Wong CH (2000) The catalytic asymmetric aldol reaction. Angew Chem Int Edit 39(8):1352–1374
29. Morris GM, Goodsell DS, Halliday RS, Huey R, Hart WE, Belew RK, Olson AJ (2007) AutoDock, Version 4.0.1, The Scripps Research Institute, La Jolla, CA, USA
30. Patel RN (2008) Synthesis of chiral pharmaceutical intermediates by biocatalysis. Coordin Chem Rev 252(5–7):659–701
31. Rashid N, Imanaka H, Imanaka T (2008) An archaeal 2-deoxyribose 5-phosphate aldolase that exhibits closer homology to bacteria rather than archaea. J Chem Soc Pakistan 30(5):740–749
32. Rydzanicz R, Zhao XS, Johnson PE (2005) Assembly PCR oligo maker: a tool for designing oligodeoxynucleotides for constructing long DNA molecules for RNA production. Nucleic Acids Res 33:W521–W525
33. Sakuraba H, Tsuge H, Shimoya I, Kawakami R, Goda S, Kawarabayasi Y, Katunuma N, Ago H, Miyano M, Ohshima T (2003) The first crystal structure of archaeal aldolase. Unique tetrameric structure of 2-deoxy-D-ribose-5-phosphate aldolase from the hyperthermophilic archaea *Aeropyrum pernix*. J Biol Chem 278(12):10799–10806
34. Sakuraba H, Yoneda K, Yoshihara K, Satoh K, Kawakami R, Uto Y, Tsuge H, Takahashi K, Hori H, Ohshima T (2007) Sequential aldol condensation catalyzed by hyperthermophilic 2-deoxy-D-ribose-5-phosphate aldolase. Appl Environ Microbiol 73(22):7427–7434
35. Sambrook J, Russell DW (2001) Molecular cloning: a laboratory manual, 3rd edn. Cold Spring Harbor Laboratory Press, Cold Spring Harbor
36. Sarethy IP, Saxena Y, Kapoor A, Sharma M, Sharma SK, Gupta V, Gupta S (2012) Alkaliphilic bacteria: applications in industrial biotechnology. J Ind Microbiol Biotechnol 38(7):769–790
37. Saw JH, Mountain BW, Feng L, Omelchenko MV, Hou SB, Saito JA, Stott MB, Li D, Zhao G, Wu JL, Galperin MY, Koonin EV, Makarova KS, Wolf YI, Rigden DJ, Dunfield PF, Wang L, Alam M (2008) Encapsulated in silica: genome, proteome and physiology of the thermophilic bacterium *Anoxybacillus flavithermus* WK1. Genome Biol 9(11):R161
38. Smith PK, Krohn RI, Hermanson GT, Mallia AK, Gartner FH, Provenzano MD, Fujimoto EK, Goeke NM, Olson BJ, Klenk DC (1985) Measurement of protein using bicinchoninic acid. Anal Biochem 150(1):76–85
39. Thompson JD, Gibson TJ, Plewniak F, Jeanmougin F, Higgins DG (1997) The CLUSTAL_X windows interface: flexible strategies for multiple sequence alignment aided by quality analysis tools. Nucleic Acids Res 25(24):4876–4882
40. Villalobos A, Ness JE, Gustafsson C, Minshull J, Govindarajan S (2006) Gene designer: a synthetic biology tool for constructing artificial DNA segments. BMC Bioinformatics 7:285
41. Wallace BA (2009) Protein characterisation by synchrotron radiation circular dichroism spectroscopy. Q Rev Biophys 42(4):317–370
42. Wang QY, Chen R, Du PF, Wu HL, Pei XL, Yang B, Yang LH, Huang LF, Liu JH, Xie T (2010) Cloning and characterization of thermostable-deoxy-D-ribose-5-phosphate aldolase from *Hyperthermus butylicus*. Afr J Biotechnol 9(20):2898–2905